

## Finite-range distorted-wave Born-approximation study of the ( ${}^4\text{He}$ , ${}^6\text{Li}$ ) reaction on ${}^{12}\text{C}$ , ${}^{24}\text{Mg}$ , and ${}^{40}\text{Ca}^\dagger$

R. G. Markham and M. A. M. Shahabuddin

Cyclotron Laboratory and Physics Department, Michigan State University, East Lansing, Michigan 48824

(Received 4 August 1976)

Angular distributions have been obtained for the ( $\alpha$ ,  ${}^6\text{Li}$ ) reaction at 46 MeV on targets of  ${}^{12}\text{C}$ ,  ${}^{24}\text{Mg}$ , and  ${}^{40}\text{Ca}$ . A finite-range distorted-wave Born-approximation analysis is performed using shell model wave functions to describe the target and various cluster wave functions to describe  ${}^6\text{Li}$ . Finite-range effects are evident in the predicted absolute magnitudes but not in the shapes of the angular distributions, which are poorly fitted. Reasonable agreement between measured and predicted absolute cross sections is obtained if the product of the  $\alpha$ - $d$  wave function and potential for the  ${}^6\text{Li}$  has no node away from the origin.

[ NUCLEAR REACTIONS  ${}^{12}\text{C}$ ,  ${}^{24}\text{Mg}$ ,  ${}^{40}\text{Ca}(\alpha, {}^6\text{Li})$ ,  $E=46$  MeV; measured  $\sigma(E_{\delta_{\text{Li}}}, \theta)$ :  
Finite-range DWBA analysis with microscopic wave functions. ]

### I. INTRODUCTION

In recent years, there has been a great deal of interest in the ( ${}^6\text{Li}$ ,  $d$ ) " $\alpha$ " transfer reaction. Studies<sup>1</sup> have found that the angular distributions have shapes which are characteristic of the transferred  $L$  and reproducible with both finite-range and zero-range distorted-wave Born-approximation (DWBA) calculations. Thus, the reaction has been very useful for making spin assignments, but so far it has only been possible to discuss the relative cross sections. The significance of the absolute cross sections is completely unknown. The prediction of absolute cross sections based on shell model wave functions requires a microscopic four nucleon form factor and a reliable reaction theory. The difficulties inherent in the construction of such a form factor and the lack of knowledge of the structure of  ${}^6\text{Li}$  [which is required in a finite-range DWBA (FRDWBA) calculation] preclude a simultaneous solution to these problems. Thus, it is necessary to isolate the two problems and solve each independently. The ( $\alpha$ ,  ${}^6\text{Li}$ )—or ( ${}^6\text{Li}$ ,  $\alpha$ )—reaction allows one to make this separation since its analysis requires the same relative motion wave function and interaction potential of the  $\alpha$  and deuteron in  ${}^6\text{Li}$  but it only requires a two nucleon form factor which is relatively well understood.

Very little data exist for either the ( $\alpha$ ,  ${}^6\text{Li}$ ) or ( ${}^6\text{Li}$ ,  $\alpha$ ) reactions. The very negative  $Q$  values ( $-15$  to  $-25$  MeV) for the ( $\alpha$ ,  ${}^6\text{Li}$ ) reaction demand a high beam energy and so the few existing experiments<sup>2</sup> have been done on light nuclei with poor resolution. Tentatively it is concluded from these works that the reaction is direct. However, Rudy *et al.*<sup>3</sup> conclude that large compound nucleus con-

tributions are present for the ( $\alpha$ ,  ${}^6\text{Li}$ ) reaction on targets of  ${}^{12}\text{C}$  and  ${}^{16}\text{O}$  at 42 MeV. On the other hand, White, Charlton, and Kemper<sup>4</sup> conclude that the  ${}^{12}\text{C}({}^6\text{Li}, \alpha){}^{14}\text{N}$  reaction is direct at  $E_{\delta_{\text{Li}}} = 33$  MeV but that multistep mechanisms may be very important. Both works included excitation functions, angular distributions and comparisons to Hauser-Feshbach calculations. The implications for  ${}^{12}\text{C}(\alpha, {}^6\text{Li})$  at 46 MeV are just not clear and, as will be demonstrated, the existing data on  ${}^{12}\text{C}$  are not able to distinguish between the different mechanisms.

Here we report a study of the ( $\alpha$ ,  ${}^6\text{Li}$ ) reaction on targets of  ${}^{12}\text{C}$ ,  ${}^{24}\text{Mg}$ , and  ${}^{40}\text{Ca}$ . Calculations are performed using FRDWBA with shell model form factors and two sets of  ${}^6\text{Li}$  cluster wave functions and potentials. The emphasis is on reproducing the absolute magnitudes of the cross sections to all states for which angular distributions have been obtained subject to the assumption of a one-step, direct transfer. Obviously, this may not be completely the case for  ${}^{12}\text{C}$  or  ${}^{24}\text{Mg}$  (due to multistep processes) but if the cross sections are even just indicative of the one-step direct contribution, we will be able to learn something about this mechanism which is vital to our understanding of the ( ${}^6\text{Li}$ ,  $d$ ) reaction.

### II. EXPERIMENT

The reactions were induced using 46 MeV  $\alpha$  particles from the Michigan State University cyclotron. Average beam intensities varied from 200 to 800 nA. The outgoing  ${}^6\text{Li}$  ions were analyzed in a split-pole spectrograph and detected in a dual proportional counter in the focal plane. The front counter was a single-wire, position-sensitive

counter using charge division readout. The second counter was operated in coincidence and served to reduce background events due to the heavy ions (such as  $^{12}\text{C}$  target recoils) which stopped in the front counter and produced pulses the same size as those of the  $^6\text{Li}$ . Otherwise, particle identification was solely by pulse height in the front counter. Because of angle-dependent path-length differences in the counter, this means of identification provided adequate separation only if the solid angle was limited to 2 msr.

The target thicknesses were  $100 \pm 10$ ,  $52 \pm 10$ , and  $371 \pm 80 \mu\text{g}/\text{cm}^2$  for  $^{12}\text{C}$ ,  $^{24}\text{Mg}$ , and  $^{40}\text{Ca}$ , respectively. These thicknesses were determined by  $\alpha$  gauge measurements for  $^{12}\text{C}$ , comparison of elastic scattering yields with thicker, known foils for  $^{24}\text{Mg}$  and energy loss measurements using the

outgoing  $^6\text{Li}$  for the  $^{40}\text{Ca}$  target. In the last case, the reaction peaks were flat topped with width determined by the target thickness and orientation. The widths of the lines were studied as a function of target angle, and the target thickness was then deduced using the known stopping powers of  $^6\text{Li}$  and  $^4\text{He}$ . Absolute cross sections were computed from integrated charge and the above target thicknesses; relative yields at the various angles were fixed in relation to a monitor detector at  $60^\circ$ . The uncertainties in the absolute cross sections are just due to the target thickness uncertainties.

Angular distributions were taken from  $11^\circ$  to  $60^\circ$  center of mass in the  $^{12}\text{C}$  experiment with the largest angle determined by the very low energy of the outgoing  $^6\text{Li}$ . (For this reaction the ground-state  $Q$  value is  $-23.7$  MeV.) The decrease of cross section with angle limited the angular range to less than  $80^\circ$  and  $55^\circ$  for  $^{24}\text{Mg}$  and  $^{40}\text{Ca}$ , respectively.

Typical spectra are shown in Fig. 1. The energy resolution in all cases was target thickness limited but adequate to resolve the low lying  $T=0$  states. There is no evidence for population of any of the low lying  $J^\pi=0^+$ ,  $T=1$  states at 1.740, 0.656, and 0.132 MeV in  $^{10}\text{B}$ ,  $^{22}\text{Na}$ , and  $^{38}\text{K}$ , respectively.

The angular distributions are shown in Fig. 2. They are most forward peaked for the  $^{40}\text{Ca}$  target where they fall off an order of magnitude from  $11^\circ$  to  $55^\circ$  and become successively less forward peaked for the lighter targets. An additional measurement was taken at  $120^\circ$  c.m. on the  $^{24}\text{Mg}$  target. The cross sections for all the states were lower by factors of 2 to 10 than the cross sections at  $60^\circ$  thus indicating a lack of symmetry about  $90^\circ$ .

### III. FRDWBA ANALYSIS

Calculations using the finite-range DWBA code "LOLA"<sup>5</sup> have been carried out. As mentioned in the Introduction such a treatment of the reaction requires a knowledge of the relative motion wave function  $\Psi_{\alpha d}$  of the  $\alpha$  and deuteron in  $^6\text{Li}$  and the interaction potential  $V_{\alpha d}$ . Specifically, the FRDWBA integrand is proportional to the product  $\Psi_{\alpha d} V_{\alpha d}$ ; hence, the reaction is sensitive to this product and not to the individual wave function and potential. We have tried two sets of wave functions and potentials. The first, to be referred to as Li1, is the Eckart function and potential with the parameters determined by Noble<sup>6</sup> ( $\epsilon=0$ ,  $R=1.5$  fm). This wave function has one node, at zero separation and the potential has an infinite repulsive core (necessary to produce the node at the origin) which perhaps may be thought of as a manifestation of the Pauli principle. The product  $\Psi_{\alpha d} V_{\alpha d}$  has a finite limiting value at zero separation and

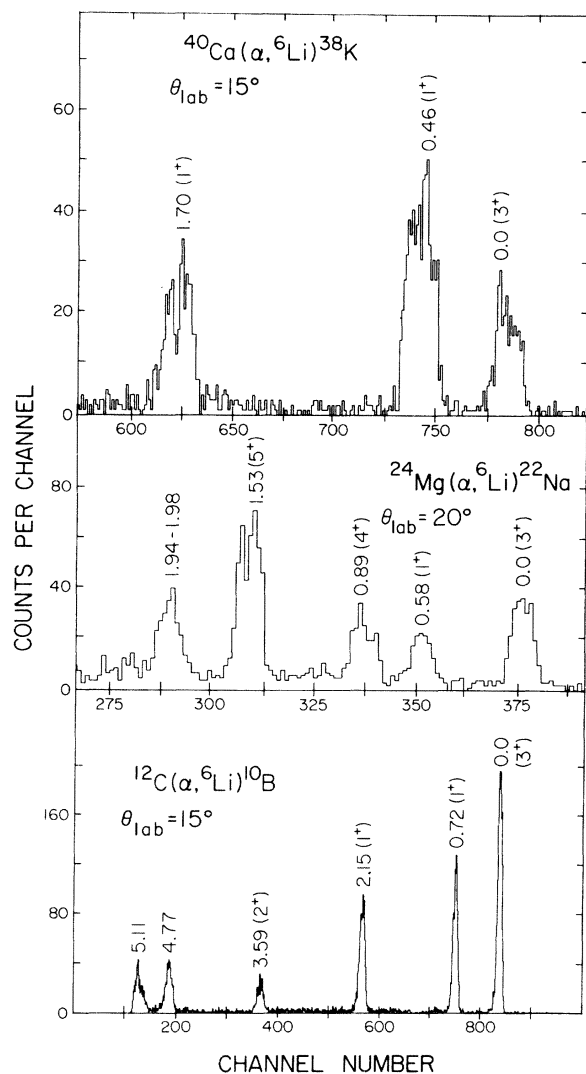


FIG. 1. Typical spectra for the three reactions studied.

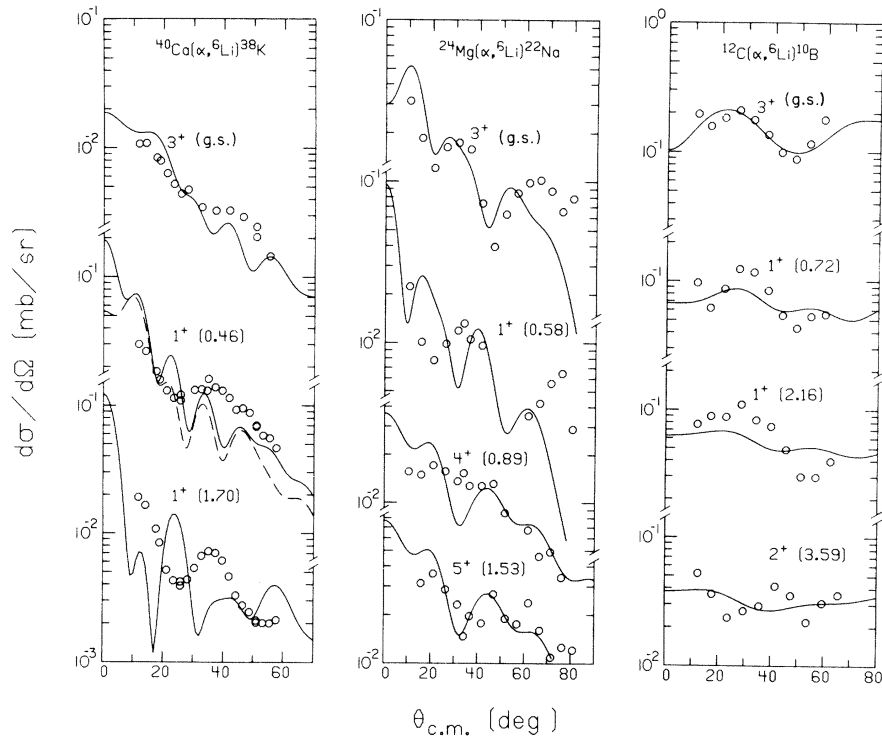


FIG. 2. Angular distributions for the three reactions. The statistical error bars (not shown) are approximately the size of the points being somewhat smaller for higher cross sections and somewhat larger for low cross sections. The curves are the result of finite range calculations. The dashed curve is the  $L=2$  contribution.

one node at about 1.1 fm. The parameters of the wave function have been derived from elastic electron scattering data and static  $M1$  and  $E2$  moments. Further, it reproduces momentum distributions obtained from  ${}^6\text{Li}(p, p\alpha)$ ,  ${}^6\text{Li}(\alpha, 2\alpha)$ , and  ${}^6\text{Li}(p, pd)$  reactions and has the proper vertex constant as concluded by Lim.<sup>7</sup>

However, there are functions (2S harmonic oscillator or Woods-Saxon) that have a node away from the origin that fit the above data equally well. Thus, we cannot be sure that  $\Psi_{\alpha d}$ , much less the product  $\Psi_{\alpha d}V_{\alpha d}$ , has the correct form. Despite the qualitative difference between the Eckart function and the 2S radial forms commonly used, the products  $\Psi_{\alpha d}V_{\alpha d}$  have a similar form (no node at the origin and one node away from the origin) and should lead to similar results in a FRDWBA calculation.

Thus, we arbitrarily chose something very different for the second wave function and potential (Li2) tried. The radial wave function chosen is similar to the Eckart function but the potential is purely attractive with a Woods-Saxon shape. This wave function is not an eigenstate of the potential. The justification for such a choice is that the Eckart function is a reasonable choice for an antisymmetrized relative motion wave function, be-

cause of the suppressed probability for both the deuteron and the  $\alpha$  being at the same place, and a purely attractive potential is not unreasonable. Here we assume that the Woods-Saxon well generates a radial wave function that after antisymmetrization of the total  ${}^6\text{Li}$  wave function has the desired shape. This is in marked contrast to the possible points of view when using the Eckart function and potential which are that the potential generates an antisymmetric form because it contains the proper exchange terms (repulsive core), or that the repulsive core is not due to the Pauli principle and that antisymmetrization of the resulting wave function does not have a significant effect.

The Li2 wave function was calculated as a bound state of a Woods-Saxon potential with a repulsive core added. This repulsive core was not used in the finite-range calculations; thus, the product  $\Psi_{\alpha d}V_{\alpha d}$  had its node at the origin. The form of the repulsive core was chosen, somewhat arbitrarily, to be equivalent to the centrifugal potential for  $L=2$  (as done by Gutbrod, Yoshida, and Bock<sup>8</sup>) and the parameters of the well (equivalent to those used by DeVries<sup>1</sup>) were chosen to produce a radial shape similar to that of the Eckart function and most nearly like that used by Jain.<sup>9</sup>

TABLE I. Optical model parameters (units are MeV and fm).

Part.	$V_R$	$r_R^a$	$a_R$	$W_V$	$W_D$	$r_I^a$	$a_I$	$r_C^a$	Ref.
$^{40}\text{Ca}(^4\text{He}, ^6\text{Li})^{38}\text{K}$									
$^4\text{He}$	162.8	1.39	0.593	20.8	...	1.54	0.589	1.25	16
$^6\text{Li}$	250.0	1.40	0.65	0	25.0	1.4	0.65	1.4	17
$p, n^b$	48.0	1.25	0.65	...	...	...	...	1.25	
$^{24}\text{Mg}(^4\text{He}, ^6\text{Li})^{22}\text{Na}$									
$^4\text{He}$	146.7	1.45	0.577	13.8	...	1.45	0.577	1.25	18
$^6\text{Li}$	262.0	1.20	0.71	16.0	...	1.75	1.15	1.4	19
$p, n^b$	62.9	1.25	0.65	...	...	...	...	1.25	
$^{12}\text{C}(^4\text{He}, ^6\text{Li})^{10}\text{B}$									
$^4\text{He}$	151.9	1.24	0.665	28.5	...	1.24	0.64	1.25	20
$^6\text{Li}$	232.0	1.25	0.755	...	6.03	2.34	0.56	2.5	21
$p, n^b$	56.9	1.25	0.65	...	...	...	...	1.25	
$^6\text{Li}$ bound state — Li2									
$\alpha-d$	39.92	1.1	0.65	...	...	...	...	1.25	$R = r(4^{1/3} + 2^{1/3})$ $E_{\alpha d} = -1.47$ MeV

<sup>a</sup>  $R = rA_T^{1/3}$  fm except as noted.

<sup>b</sup> The well depths were not varied from state to state.

The target form factors were generated microscopically from single-particle wave functions according to the technique of Bayman and Kallio.<sup>10</sup> The protons and neutrons were bound in the same potential well chosen so that the sum of the proton and neutron binding energies for the lowest valence orbit would be equal to the deuteron separation energy for the ground state. The two nucleon parentage amplitudes for the  $^{40}\text{Ca}$  and  $^{24}\text{Mg}$  experiments were taken from two different sets of shell model wave functions.<sup>11-14</sup> For the  $^{12}\text{C}$  experiment, the wave functions of Cohen and Kurath<sup>15</sup> were used.

To extract the ratio of experiment to theory it was assumed that the  $^6\text{Li}$  had unit probability of being in an  $\alpha$  plus deuteron state.

Many optical model parameters were tried with greatly varying degrees of success. The sets we found most suitable are listed in Table I. The criteria for whether a set of parameters was acceptable or not was the fit to the shapes of the angular distributions with each target being considered separately.

#### IV. ANGULAR DISTRIBUTIONS

The results of the finite-range calculations using Li2 for the  $^6\text{Li}$  wave function and potential and using shell model form factors are shown in Fig. 2. The curves are the sum of the allowed  $L$  transfers and each curve is independently normalized to the data. The calculations using Li1 for the  $^6\text{Li}$  wave function and potential gave very similar angu-

lar distributions and so are not shown. In all but one case, the theoretical curves are dominated by a single  $L$  transfer; for that case, the most significant contributing  $L$  is also plotted. The factors needed to normalize the theory to the data are listed in Table II; ideally, they should be about equal to 1. However, the absolute magnitudes are very different for the two calculations.

TABLE II. Ratios of experimental to theoretical and theoretical to theoretical cross sections.

Target	$J^\pi$	$E_x$	Experiment/Theory			Theory ratio <sup>c</sup>
			Li2 <sup>a</sup>	Li2 <sup>b</sup>	Li1 <sup>b</sup>	
$^{40}\text{Ca}$	3 <sup>+</sup>	0	0.75	0.74	28	38
	1 <sup>+</sup>	0.46	2.04	1.54	49	32
	1 <sup>+</sup>	1.70	1.83	2.17	44	20
$^{24}\text{Mg}$	3 <sup>+</sup>	0	4.36	4.25	291	68
	1 <sup>+</sup>	0.58	7.71	4.24	254	60
	4 <sup>+</sup>	0.89	153	71	4417	62
	5 <sup>+</sup>	1.53	14	19	1239	65
$^{12}\text{C}$	3 <sup>+</sup>	0		0.89	18	20
	1 <sup>+</sup>	0.72		0.30	6	20
	1 <sup>+</sup>	2.15		0.63	13	21
	2 <sup>+</sup>	3.58		1.70	30	18

<sup>a</sup> The shell model wave functions used are from Ref. 11 for  $^{38}\text{K}$  and Ref. 12 for  $^{22}\text{Na}$  and  $^{24}\text{Mg}$ .

<sup>b</sup> The shell model wave functions used are from Ref. 13 for  $^{38}\text{K}$ , from Ref. 14 for  $^{22}\text{Na}$  and  $^{24}\text{Mg}$  and from Ref. 15 for  $^{10}\text{B}$  and  $^{12}\text{C}$ .

<sup>c</sup> Ratio of column 6 to column 5. The ratio  $D_0^2(\text{Li2})/D_0^2(\text{Li1}) = 16.5$ .

#### A. $^{40}\text{Ca}(\alpha, ^6\text{Li})^{38}\text{K}$ reaction

Two sets of shell model wave functions for  $^{38}\text{K}$  were tried. In both cases,  $^{40}\text{Ca}$  was taken as the closed core so the  $^{38}\text{K}$  wave functions differ only in the choice of two body interaction. The predicted cross sections are the same within 30% and the angular distributions are little affected.

The ground state is populated by an almost pure  $L=4$  transfer. The shape of the angular distributions is rather well reproduced but the theory predicts too many small oscillations. This is more apparent for the first excited  $J^\pi=1^+$  state which is populated by a mixture of  $L=0$  and 2. No combination of these  $L$  transfers can remove the oscillations implying that the problem is due to the choice of parameters for the optical model or bound states.

The measured angular distribution for the second excited  $J^\pi=1^+$  state is very similar to the one for the first excited state. The shell model predicts it to be excited by an almost pure  $L=0$  transfer, but this apparently is not the case. Furthermore the cross sections for  $J^\pi=1^+$  states are relatively underpredicted compared with the ground state. Thus, we feel that the shell model is the source of difficulty here and in particular the difficulty may be related to the assumed shell closure at  $^{40}\text{Ca}$ .

#### B. $^{24}\text{Mg}(\alpha, ^6\text{Li})^{22}\text{Na}$ reaction

Two sets of shell model wave functions for  $^{24}\text{Mg}$  and  $^{22}\text{Na}$  were tried. The first set was constructed in a truncated model space and the second in the full  $s$ - $d$  shell. Again both sets gave similar angular distributions (only the predictions using the full space are shown in Fig. 2).

Again the ground-state angular distribution is well reproduced, but in this case the transfer is almost pure  $L=2$  in character. The first excited  $J^\pi=1^+$  state is poorly fitted by the predicted  $L=0$  transfer. The shape of the  $J^\pi=1^+$  angular distribution strongly resembles the ground-state  $L=2$  shape and so we feel it is largely populated by  $L=2$ . Both sets of shell model wave functions predict the dominance of the  $L=0$  component, but this transition is the most sensitive to the change of model space.

The  $J^\pi=4^+$  and  $5^+$  states can only be populated by  $L=4$  transfer. The shapes of the angular distributions are well reproduced particularly for the  $J^\pi=5^+$  state. However, the cross sections are underpredicted by large factors. Both transitions are quite sensitive to the choice of shell model wave functions, but because of the size of the discrepancy, the prospect that additional reaction channels are important must be considered.

Recently a  $^{24}\text{Mg}(d, \alpha)^{22}\text{Na}$  experiment<sup>22</sup> has been reported. In this work poor agreement was found for the  $J^\pi=1^+$  state and the  $J^\pi=4^+$  state was populated 10 times stronger than predicted. The two experiments seem to be quite consistent but at serious odds with the theory. This could readily be attributed to a failure of the shell model, but it is also likely that two-step processes would affect both reactions in a similar manner.<sup>23</sup> One cannot be certain which is at fault. A favored two step route for excitation of the  $J^\pi=4^+$  and  $5^+$  states would be pickup to the  $J^\pi=3^+$  ground state followed by inelastic excitation since these states are believed to be part of a rotation band. If such were the case then the  $J^\pi=4^+$  state (and in some measure the  $J^\pi=5^+$  state) are made dominantly by two-step transfer. However, the ground-state and  $J^\pi=1^+$  state cross sections may well give a reasonable indication of the magnitude of the one-step cross section, since although the two-step cross section may seriously affect relative cross sections to various states it is not likely to cause an overall drastic enhancement for all states.

#### C. $^{12}\text{C}(\alpha, ^6\text{Li})^{10}\text{B}$ reaction

The shell model wave functions of Cohen and Kurath<sup>14</sup> were used to describe the states of  $^{10}\text{B}$  and  $^{12}\text{C}$ . The ground-state angular distribution is fitted very well by the predicted  $L=2$  angular distribution. The fits to the first and second excited  $J^\pi=1^+$  states are less satisfactory with the predicted angular distributions becoming too flat with increased excitation energy. In this instance, both  $J^\pi=1^+$  states are predicted to be dominantly  $L=0$  transfers.

The  $J^\pi=2^+$  state at 3.59 MeV is seen only weakly and has a rather structureless angular distribution. The predicted  $L=2$  angular distribution, also rather flat, seems to be out of phase with the data. The energy in the center of mass is quite low in the outgoing channel for these excited states so that an energy-independent optical model might not reproduce the  $Q$ -value dependence of the reaction.

As mentioned earlier there may well be a large contribution to the cross section from the compound nucleus mechanism. The best evidence to this effect is the work of Rudy *et al.*,<sup>3</sup> at 42 MeV. At 46 MeV we expect the direct contribution to be only about 50% larger hence our conditions are only somewhat more favorable. However, it is doubly difficult to distinguish between compound and direct in this case because the usual indicators are unreliable. As can be seen in Fig. 3, the direct yields are not lower at back angles so that one cannot assume that the  $180^\circ$  cross section is

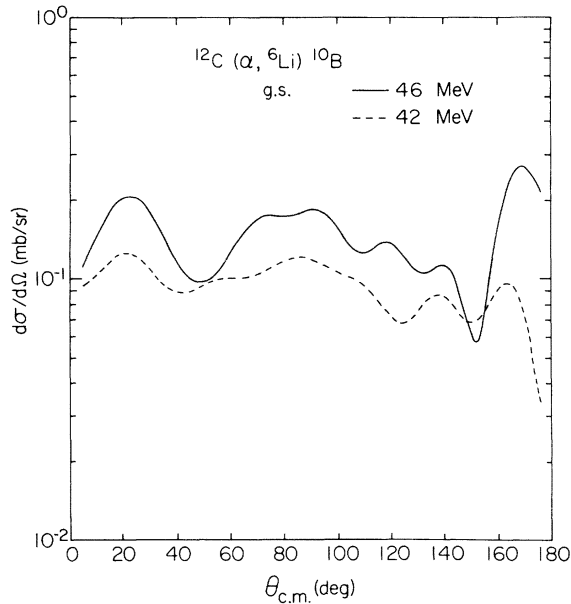


FIG. 3. Finite-range calculations for 46 and 42 MeV using the Li2 lithium wave function and potential and the parameters of Table I. The curves were multiplied by 0.9 to reproduce the 46 MeV data.

a measure of the compound contribution. Excitation functions at fixed angles are also unreliable. With the parameters of our calculations held fixed and the incident energy varied we find a ground-state,  $0^\circ$  excitation function which fluctuates. These fluctuations are much like those observed by Seale,<sup>24</sup> in terms of amplitude, although they have about twice the width. Unfortunately DWBA predictions of excitation functions also are not reliable because of the lack of accurate, energy-dependent optical parameters. As mentioned earlier, White *et al.*<sup>4</sup> conclude that the  $^{12}\text{C}(^6\text{Li}, \alpha)^{14}\text{N}$  reaction is direct at  $E_{^6\text{Li}} = 33$  MeV. The  $^6\text{Li}$  energies in the present work are half as large, hence we cannot draw any inferences.

The best evidence for direct contributions to the reaction at 46 MeV lies in the asymmetry of the angular distributions of Rudy and the structure of the angular distributions observed in the present work. Thus it is reasonable to assume that the reaction is, in some measure, direct.

#### V. ABSOLUTE CROSS SECTIONS

In general, the agreement between theory and experiment is good when the Li2 wave function and potential is used. If we ignore the  $J^\pi = 4^+$  and  $5^+$  states of  $^{22}\text{Na}$ , we find that the ratio of experimental to theoretical cross sections varies from 0.3 to 4.2 for Li2 and from 6 to 291 for Li1. Not only are these ratios much closer to unity for Li2;

but also, they are more nearly constant. The  $^{12}\text{C}$  data support the preference for Li2 as long as this reaction is mostly direct in the angular range studied.

The ratio of Li2 to Li1 cross sections for all states are tabulated in the last column of Table II. These ratios show that the Li1 cross sections are both considerably smaller (factors of 18 to 68) and not simply related to the Li2 cross sections as would be expected if the zero-range approximation were valid (the ratio of  $D_0^2$  for Li2 to  $D_0^2$  for Li1 is 16.5).

A probable explanation is that the presence of a node in the product of the wave function and potential for Li1 makes it possible for the positive and negative portions of the product to give canceling contributions to the DWBA integral. The degree of cancellation will clearly depend on the position of the node, on the shape of the wave function and potential and on all of the other parameters of the calculation. A demonstration of the dependence of the cross section on the node position is shown in Fig. 4. This figure shows the relative  $0^\circ$  cross

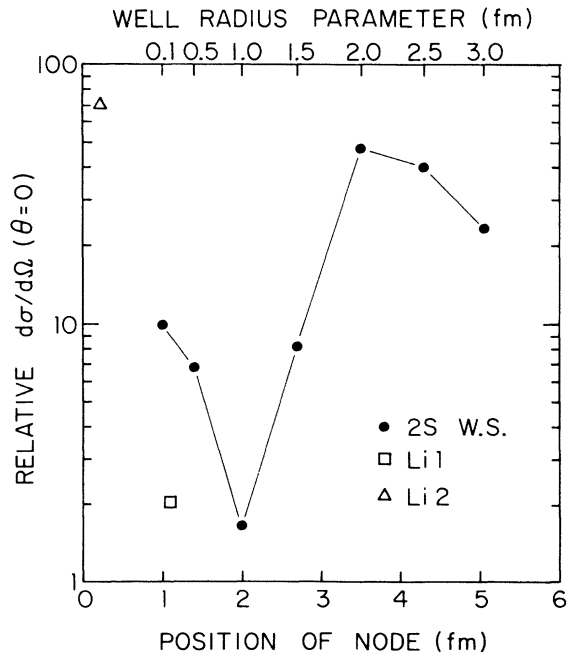


FIG. 4. Relative  $0^\circ$  cross sections for the  $L=0$  component of the first  $J^\pi = 1^+$  state of  $^{38}\text{K}$  plotted as a function of node position. For these calculations, a 2S solution of a Woods-Saxon well was used. The binding energy was held fixed at 1.47 MeV and the geometry was  $a_r = 0.65$ ,  $R_c = R_R = r_0(4^{1/3} + 2^{1/3})$  with  $r_0$  varied from 0.1 to 3.0 fm. The line serves only to connect the calculated points. The corresponding magnitudes for Li1 and Li2 are indicated.

sections for the  $L=0$  contribution to the first  $J^\pi = 1^+$  state of  $^{38}\text{K}$  as a function of node position (and well radius parameter). The wave functions and potentials were obtained by searching on the well depths of Woods-Saxon wells of various radii to produce 2S radial wave functions of the proper binding energy. Notice there is a very localized and dramatic decrease of the cross section near a node position of 2 fm. If the node is taken at very large radii ( $>3$  fm), the cross section increases to somewhat less than the Li2 cross section. Likewise the cross sections become more near agreement with experiment for node positions close to zero but for this 2S form the Woods-Saxon well must have an unphysically small radius.

From this we conclude that the product of the  $^6\text{Li}$  wave function and potential is unlikely to have a node except possibly at zero separation. A similar conclusion was reached by Gutbrod *et al.*<sup>8</sup> in an analysis of the ( $d, ^6\text{Li}$ ) reaction of  $p$  and  $s$ - $d$  shell targets. They observed that the 2S radial form with a Woods-Saxon well vastly overestimated the decrease of cross section with increasing target mass. We do not observe this same phenomenon, but such an effect would be sensitive to the other details of the reaction.

## VI. SUMMARY

The ( $\alpha, ^6\text{Li}$ ) reaction seems to proceed partly via a simple direct mechanism with the angular distributions being forward peaked and isospin being conserved. However, the  $J^\pi = 4^+$  and  $5^+$  states in  $^{22}\text{Na}$  are populated with anomalously large cross sections which suggests the possible importance of other reaction channels. Also, it is likely that compound nucleus formation is important for  $^{12}\text{C}$ .

The shapes of the angular distributions are sensitive to the optical model parameters and insensitive to the choice of  $^6\text{Li}$  wave function or interaction. The quality of the fits varied greatly depending most on the ability of the shell model to predict the proper ratio of  $L$  transfers. The most difficulty was encountered with  $J^\pi = 1^+$  states. The predicted absolute magnitudes were found to be very sensitive to the  $^6\text{Li}$  wave function and potential. This sensitivity was traced to cancellations in the integration caused by the presence of a node at  $r > 0$  in the product  $V_{\alpha d}\Psi_{\alpha d}$ . Comparison to the data supports the placement of the node at zero separation. With such a wave function and potential the absolute cross sections are well reproduced.

<sup>†</sup>Work supported by the National Science Foundation.

<sup>1</sup>H. W. Fulbright, U. Strohbush, R. G. Markham, R. A. Lindgren, G. C. Morrison, S. C. McGuire, and C. L. Bennett, Phys. Lett. **53B**, 449 (1975); R. M. DeVries, H. W. Fulbright, R. G. Markham, and U. Strohbush, *ibid.* **55B**, 33 (1975).

<sup>2</sup>C. D. Zafiratos, Phys. Rev. **136**, B1279 (1964); P. F. Mizera and J. B. Gerhart, *ibid.* **170**, 839 (1968); B. Zeidman, H. T. Fortune, and A. Richter, Phys. Rev. **C 2**, 1612 (1970).

<sup>3</sup>C. Rudy, R. Vanderbosch, P. Russo, and W. J. Braithwaite, Nucl. Phys. **A188**, 430 (1972).

<sup>4</sup>R. L. White, L. A. Charlton, and K. W. Kemper, Phys. Rev. **C 12**, 1918 (1975).

<sup>5</sup>R. M. DeVries, Phys. Rev. **C 8**, 951 (1973).

<sup>6</sup>J. V. Noble, Phys. Rev. **C 9**, 1209 (1974).

<sup>7</sup>T. K. Lim, Phys. Lett. **56B**, 321 (1975).

<sup>8</sup>H. H. Gutbrod, H. Yoshida, and R. Bock, Nucl. Phys. **A165**, 240 (1971).

<sup>9</sup>A. K. Jain, J. Y. Grossiord, M. Chevallier, P. Gaillard, A. Guichard, M. Gusakow, and J. R. Pizzi, Nucl. Phys. **A216**, 519 (1973).

<sup>10</sup>B. F. Bayman and A. Kallio, Phys. Rev. **156**, 1121 (1967).

<sup>11</sup>B. H. Wildenthal, E. C. Halbert, J. B. McGrory, and T. T. S. Kuo, Phys. Rev. **C 4**, 1266 (1971).

<sup>12</sup>B. M. Preedom and B. H. Wildenthal, Phys. Rev. **C 6**, 1633 (1972); J. B. McGrory and B. H. Wildenthal, Phys. Lett. **34B**, 373 (1971).

<sup>13</sup>B. H. Wildenthal and W. Chung (unpublished).

<sup>14</sup>B. H. Wildenthal and W. Chung (unpublished).

<sup>15</sup>S. Cohen and D. Kurath, Nucl. Phys. **A101**, 1 (1967).

<sup>16</sup>D. F. Jackson and C. G. Morgan, Phys. Rev. **175**, 1402 (1968).

<sup>17</sup>U. Strohbush (private communication).

<sup>18</sup>L. McFadden and G. R. Satchler, Nucl. Phys. **84**, 177 (1966).

<sup>19</sup>V. I. Chuev, V. V. Davidov, B. G. Navatskii, A. A. Ogloblin, S. B. Sakuta, and D. N. Stepanov, J. Phys. (Paris) **C6**, 157 (1971).

<sup>20</sup>P. Gaillard, R. Bouche, L. Feuvrais, M. Gaillard, A. Guichard, M. Gusakow, J. L. Leonhardt, and J. R. Pizzi, Nucl. Phys. **A131**, 353 (1969).

<sup>21</sup>J. W. Watson, Nucl. Phys. **A198**, 129 (1972).

<sup>22</sup>M. J. Schneider and J. W. Olness, Phys. Rev. **C 13**, 1392 (1976).

<sup>23</sup>C. H. King (private communication).

<sup>24</sup>W. A. Seale, Phys. Rev. **160**, 809 (1967).